JOURNAL OF CATALYSIS **173,** 134–144 (1998)
ARTICLE NO. CA971898

Molybdenum Nitride and Carbide Prepared from Heteropolyacid

II. Hydrodenitrogenation of Indole

Senzi Li and Jae Sung Lee[1]

Department of Chemical Engineering and School of Environmental Engineering, Pohang University of Science and Technology, Pohang 790-784, Republic of Korea

Received March 24, 1997; revised August 4, 1997; accepted September 8, 1997

Hydrodenitrogenation (HDN) of indole has been studied over Mo_2N prepared from MoO_3, 12-molybdophosphoric acid (HPA) and $MoO_3 + P_2O_5$ (a physical mixture of P_2O_5 and MoO_3 with stoichiometry of P to Mo equal to that of HPA). It has been observed that Mo_2N is an active catalyst for HDN of indole. It gave comparable activity (per unit mass) to that of Mo–Ni/γ-Al_2O_3 but less hydrogen consumption. The initial activity of indole HDN was significantly increased by adding phosphorus in the catalysts despite its unfavorable pore and site blocking effects. However, P-containing Mo_2N lost activity more readily than Mo_2N itself. The deactivation did not result from carbon but probably was caused by nitrogen deposits from indole and loss of surface area. The bulk structure and morphology of the Mo_2N catalysts were not changed after HND of indole. The reaction pathway did not appear to be altered by adding phosphorus.

INTRODUCTION

Hydrodenitrogenation (HDN), which occupies a significant position in petroleum refining industry, is a hydrotreating process aimed at reducing the nitrogen content of crude. It makes easier the downstream processing to commercially useful products and environmentally acceptable fuels. Sulfided Ni(Co)–Mo/Al_2O_3 have been commercially used for more than half a century as catalysts due to their reliable activity and thermal resistance in spite of the fact that many attempts have been made to substitute alumina with other supports such as active carbon, metal oxides and zeolites. Commercial hydrotreating catalysts usually contain a small portion of phosphorus as an additive. A number of patents claimed the promotional effects of phosphorus, including promoting dispersion of metal, altering surface acidity, modifying morphology and increasing thermal stability of catalysts (1–4). Although a few papers reported negative effects of phosphorus over Mo/carbon catalysts (5, 6), most publications gave favorable examples of phosphorus for HDN and hydrodesulfurization (HDS) reactions over Mo-based alumina supported catalysts (7–16). It has been proposed that phosphate has a strong affinity with alumina while weakening the interaction between molybdenum and support. However, a clear understanding of the role of phosphorus has not yet been achieved.

Recently, much attention has been paid to molybdenum carbide or nitride (17–20) which has shown encouraging activity in noble metal catalyzed reactions as well as HDN and HDS (21–27). However, to the best of our knowledge, no report concerns the influence of phosphorus in unsupported molybdenum carbide or nitride for HDN reaction. The study presented here takes advantage of both systems. First, high surface area Mo_2N, which consists totally of active material unlike commercial supported catalysts in which the support itself occupies a large volume, is applied to HDN of indole. It can improve the catalytic efficiency and simplify the system. Second, phosphorus coming from different precursors is introduced into Mo_2N to gain a better understanding of the function of phosphorus in the system. On the basis of previous preparation and characterization results (32), this work evaluates the activity of indole HDN over Mo_2N prepared from MoO_3, 12-molybdophosphoric acid (a heteropolyacid, HPA) and $MoO_3 + P_2O_5$ (a physical mixture of P_2O_5 and MoO_3 with stoichiometry of P to Mo equal to that of HPA). These systems are expected to present an opportunity to get further insight into the role of phosphorus in HDN reaction.

EXPERIMENTAL

Catalyst Preparation

All of the catalysts were prepared by temperature-programmed reaction of MoO_3, $MoO_3 + P_2O_5$ or 12-molybdophosphoric acid (HPA) with ammonia. The detailed synthesis and characterization results have been described in the previous paper (32). Typically 0.01 mol precursors were employed and a stream of NH_3 at a flow rate of 150 μmols^{-1} was passed through the reaction cell at

[1] To whom correspondence should be addressed. Fax: 82-562-279-5799. E-mail: jlee@vision.postech.ac.kr.

0021-9517/98 $25.00

atmospheric pressure. Temperature of the preparation was increased linearly at a rate of 30 Kh^{-1} between 573 and 973 K.

Mo–Ni/γ-Al_2O_3 containing 13.2 wt% MoO_3 and 2.7 wt% NiO was prepared by a wet impregnation method according to the composition of commercial Shell 324 catalyst. Calculated amounts of aqueous solution of ammonium heptamolybdate and nickel nitrate were added to γ-Al_2O_3 (Aldrich, 99.5%, surface area of 150 $m^2\,g^{-1}$, pore volume of 0.5 $cm^3\,g^{-1}$). Water was removed in rotary evaporator under vacuum at 330 K. Then, the catalyst was dried in an oven at 400 K for 12 h and then calcined at 773 K in air for 3 h prior to the HDN reaction.

Hydrodenitrogenation of Indole

Indole, representative of nitrogen compounds in crude oil, was chosen as the model compound to test the hydrodenitrogenation (HDN) activity of catalysts. 1.03 g Mo_2N was prepared from different precursors and used for each activity measurement. HDN of indole was carried out *in situ* without exposing the catalysts to air after preparation. The catalysts were pretreated under the flow of hydrogen at a rate of 15 $\mu mols^{-1}$ at 673 K for 1 h just prior to the delivery of indole. Indole (Aldrich, 99+%) was introduced into the flow of hydrogen (90 $\mu mols^{-1}$) via a syringe pump (Saga Instruments) at a pumping rate of 0.1 $cm^3\,h^{-1}$ at atmospheric pressure. A vaporization chamber filled with glass beads was positioned upstream of quartz reactor to ensure a complete mixing of gases. Identification and analysis of reaction products were carried out by an on-line HP 5890 gas chromatography (GC) equipped with an FID detector and by mass spectroscopy. An STB-1 capillary column (60 m $\times$ 0.25 mm $\times$ 0.25 μm) of Supelco was used to separate products for GC analysis.

The hydrodenitrogenation of indole as a function of reaction temperature was performed following a temperature ramping program from 573 to 773 K. The temperature was maintained at the indicated temperature for 2 h prior to moving to the next temperature level at a ramping rate of 0.083 Ks^{-1}. The effluent products were analyzed every 20 min via a six-port sampling valve attached on GC. The average value of the last three samplings was taken as activity data of the indicated temperature since deactivation occurred with time on stream. The value of error for the average was ca. $\pm$5%.

Characterization of Catalysts

Since fresh molybdenum carbide and nitride were burned violently with flame upon exposure to air, the samples were passivated prior to the characterization measurements by letting air diffuse slowly into the reaction cell with one end of the reactor open to atmosphere for 10 h and causing a mild surface oxidation.

The specific surface areas S_g of the samples were determined on a constant volume adsorption apparatus (Micrometrics ASAP 2021C) by the N_2 BET method. Power X-ray diffraction (XRD) measurements were conducted using a Mac Science M18XHF diffractometer with Cu Kα_1 radiation. Carbon content of the catalysts after HDN reaction was determined by a CS-444 carbon/sulfur analyzer (Leco).

The morphology of passivated samples before and after HDN reaction was observed by scanning electron microscopy (SEM) on a Jeol JSM-840A. The lateral distributions of P in Mo_2N prepared from $MoO_3 + P_2O_5$ and HPA were determined by electron probe microanalysis (EPMA) with wavelength-dispersive spectroscopy (WDS) on Jeol JXA-8600. For these analyses, samples were mounted on graphite stubs and gold was sputtered onto them to ensure an adequate conductivity.

X-ray photoelectron spectroscopy (XPS) measurements were conducted using Perkin-Elmer PHI 5400 ESCA spectrometer with monochromatic Mg Kα radiation (1253.6 eV) at 15 kV and 20 mA. About 0.2 g catalysts in a passivated form were pressed into a pellet at 34 MPa for the measurement. The spectrometer energies were calibrated using Au $4f_{1/2}$ peak at 84.0 eV, Ag $3d_{5/2}$ at 368.0 eV and Cu $2p_{3/2}$ at 932.6 eV. Vacuum in the measurement chamber during the collection of spectra was maintained below 5×10^{-9} torr. Spectra were collected with an analyzer pass energy of 89.45 eV for survey scan and 71.55 eV for individual element range. In order to obtain reproducible results, a strict standardization of the order and the time of recording was used. Charging effect was circumvented by referencing binding energies to that of C_{1s} peak at 285.0 eV. Overlapping peaks were deconvoluted using a curve fitting procedure based on non-linear-least-square algorithm (28). Depth profiles were obtained by bombardment of Ar^+ ion on the samples at a sputtering rate of 2 nm per minute for 12 cycles until 20 nm surface was removed.

RESULTS

Hydrodenitrogenation of Indole over Mo_2N Prepared from Different Precursors

Figure 1 shows the rates of indole HDN reaction as a function of temperature for the same weight of catalyst. It was observed that Mo_2N is an active catalyst for HDN of indole. It gave comparable reaction rates to those of Mo–Ni/γ-Al_2O_3 on the same weight basis. It was found that at 773 K nearly all of indole was converted to hydrocarbons. Over the temperature range lower than 723 K, Mo_2N prepared from P-containing precursors showed higher reaction rates than that from MoO_3. This trend was especially evident in the case of HPA-derived Mo_2N. However, these higher rates of P-containing catalyst disappeared at temperatures higher than 723 K.

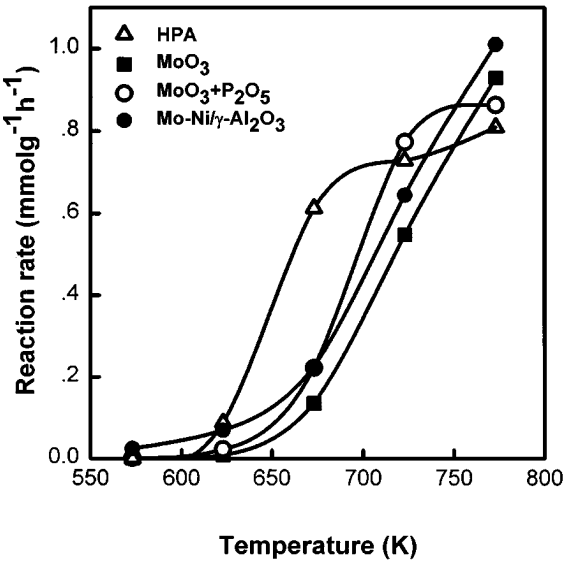

FIG. 1. Catalytic activity as a function of temperature over Mo_2N prepared from different precursors and Mo–Ni/γ-Al_2O_3. (Indole feeding rate = 0.1 cm^3 h^{-1}, H_2 flow rate = 90 μmols^{-1}, catalyst loading = 1.03 g.)

The products of indole HDN reaction could be classified into three groups: hydrogenolysis of C–N in heterocyclic ring results in aniline group compounds of aniline, methylaniline and ethylaniline still containing N. Further hydrogenolysis of C–N bonds leads to aromatic hydrocarbon products such as benzene, toluene and ethylbenzene. Hydrogenation and hydrogenolysis of the benzene ring yields low molecular weight saturated hydrocarbon products. Figures 2 and 3 show distributions of aniline and hydrocarbon group products, respectively. It was found that the weight percentage of aniline group products increased with increasing reaction temperature and then declined dramatically at temperatures higher than 673 K. Meanwhile the weight percentage of hydrocarbon group products increased with increasing reaction temperatures except the amount of ethylbenzene that decreased at higher temperatures for Mo_2N catalysts. It is worth noting that similar temperature dependence of product distributions was obtained regardless of precursors although that of HPA-derived Mo_2N shifted to ca. 50 K lower temperatures than those of the other two catalysts.

It is worthy to mention that all Mo_2N catalysts prefer hydrodenitrogenation to hydrogenation of aromatic ring when compared to Mo–Ni/γ-Al_2O_3 catalysts. As shown in Fig. 3(a), the formation of saturated hydrocarbons over Mo–Ni/γ-Al_2O_3 catalysts was substantially higher than those from Mo_2N catalysts, especially at high temperatures. The lower hydrogen consumption for Mo_2N catalysts is of great economic significance in industrial hydrotreating processes.

In addition, indole HDN reaction was carried out at 673 K over three samples and the reaction rates were monitored with time on stream (Fig. 4). P-containing Mo_2N showed higher activities at the beginning of the reaction, while they decreased significantly as reaction proceeded, particularly in the case of HPA-derived Mo_2N. In contrast, Mo_2N prepared from MoO_3 deactivated only slightly with time. The product distributions with time on stream over Mo_2N prepared from MoO_3 and $MoO_3 + P_2O_5$ were similar while that over HPA-derived Mo_2N was somewhat different (Figs. 5, 6). In the latter case, the content of toluene decreased rapidly whereas methylaniline and ethylaniline increased with time and then decreased markedly after 10 h on stream.

Characterization of the Catalysts after Indole HDN Reaction

The surface areas of Mo_2N prepared from different precursors after 10 h run are summarized in Table 1. The surface area of all the catalysts decreased after indole HDN reaction. The addition of P_2O_5 to MoO_3 resulted in a decrease of Mo_2N surface area of ca. 30% while HDN reaction led to an additional 30% decrease of its surface area. In the case of HPA, the initial surface area was much smaller than

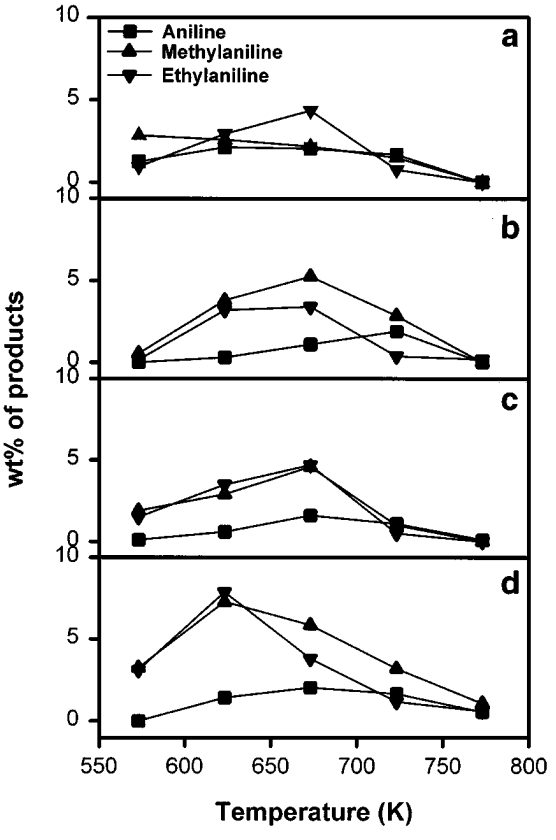

FIG. 2. Product distribution of aniline group compounds as a function of temperature over (a) Mo–Ni/γ-Al_2O_3 and Mo_2N prepared from (b) MoO_3, (c) $MoO_3 + P_2O_5$, and (d) HPA. (Indole feeding rate = 0.1 cm^3 h^{-1}, H_2 flow rate = 90 μmols^{-1}, catalyst loading = 1.03 g.)

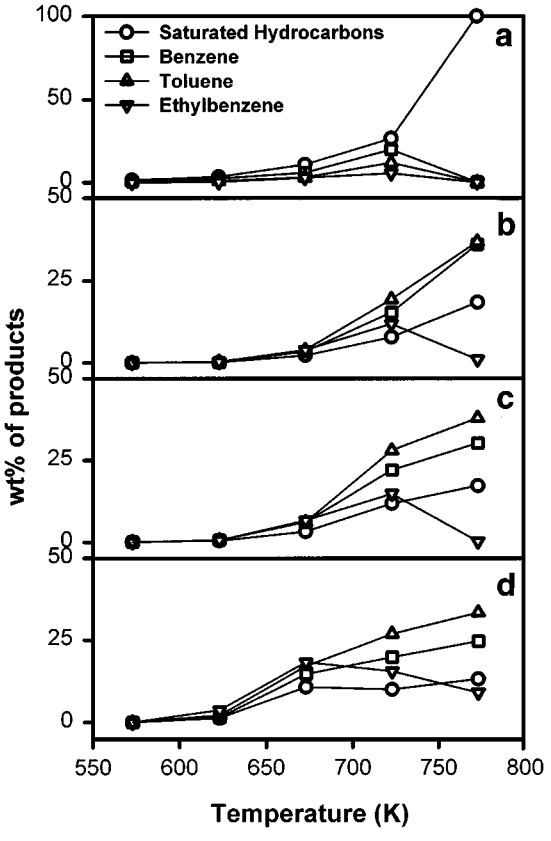

FIG. 3. Product distribution of hydrocarbon group compounds as a function of temperature over (a) Mo–Ni/γ-Al_2O_3 and Mo_2N prepared from (b) MoO_3, (c) $MoO_3 + P_2O_5$, and (d) HPA. (Indole feeding rate = 0.1 $cm^3\ h^{-1}$, H_2 flow rate = 90 $\mu mols^{-1}$, catalyst loading = 1.03 g.)

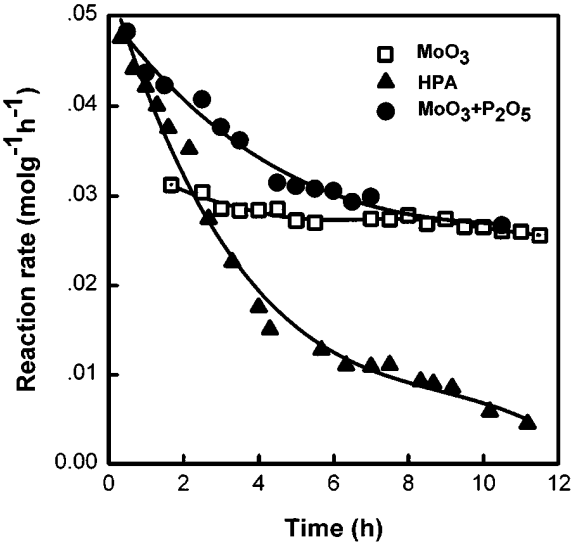

FIG. 4. Catalytic activity with time on stream over Mo_2N prepared from different precursors. (Indole feeding rate = 0.1 $cm^3\ h^{-1}$, H_2 flow rate = 90 $\mu mols^{-1}$, catalyst loading = 1.03 g, reaction temperature = 673 K.)

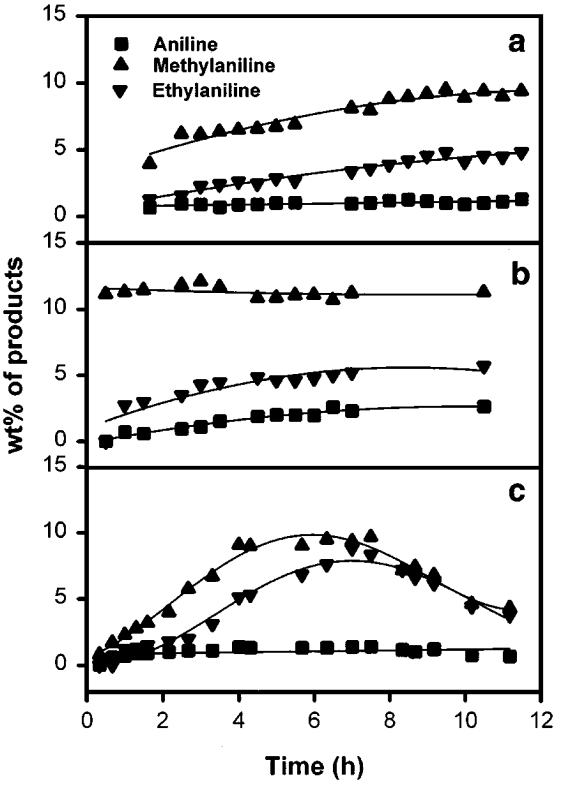

FIG. 5. Product distribution of aniline group compounds with time on stream over Mo_2N prepared from (a) MoO_3, (b) $MoO_3 + P_2O_5$, and (c) HPA. (Indole feeding rate = 0.1 $cm^3\ h^{-1}$, H_2 flow rate = 90 $\mu mols^{-1}$, catalyst loading = 1.03 g, reaction temperature = 673 K.)

the other two samples and ca. 50% of it was lost during the reaction. Carbon contents of the catalysts after indole HDN reaction are also listed in Table 1. There was no appreciable difference in the carbon content among these samples.

The catalysts were removed from the reactor after reaction and analyzed by X-ray diffraction (Fig. 7). Peak location and diffraction intensity show that γ-Mo_2N with face-centered-cubic structure was formed regardless of the precursors and the bulk structure of Mo_2N was maintained even after 10 h of the reaction at 673 K.

The SEM images of fresh catalysts have been reported in the previous publication (32). As seen from SEM images

TABLE 1

Characteristics of Mo_2N Catalysts Prepared from Different Precursors

Precursors	MoO_3	$MoO_3 + P_2O_5$	HPA
Specific surface area/$m^2\ g^{-1}$			
Before reaction	123.1	90.6	21.0
After reaction[a]	94.1	74.2	9.1
Carbon content/wt%			
After reaction[a]	0.78	0.86	0.85

[a] Hydrodenitrogenation of indole at 673 K for 10 h.

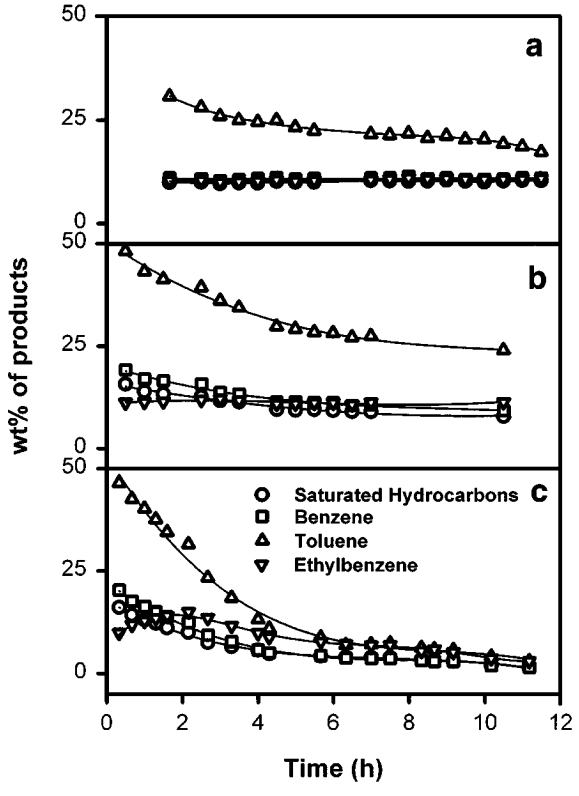

FIG. 6. Product distribution of hydrocarbon group compounds with time on stream over Mo_2N prepared from (a) MoO_3, (b) $MoO_3 + P_2O_5$, and (c) HPA. (Indole feeding rate = 0.1 $cm^3 h^{-1}$, H_2 flow rate = 90 $\mu mols^{-1}$, catalyst loading = 1.03 g, reaction temperature = 673 K.)

of used catalysts, the morphology of Mo_2N remained unchanged (Figs. 8a and 9a) after HDN of indole at 673 K for 10 h. The lateral distribution of P after HDN reaction analyzed by EPMA over Mo_2N prepared from $MoO_3 + P_2O_5$ (Fig. 9b) was not homogeneous. There were some discrete particles of P as indicated by the clusters of especially bright white spots that had no correlation with morphology of Mo_2N particles seen by SEM. In contrast, P distribution in HPA-derived Mo_2N was quite uniform (Fig. 8b). When compared to P distribution in fresh Mo_2N reported in the companion paper (32), the distribution of P seemed not altered after HND of indole.

The change of binding energy and intensity upon XPS depth profile enables us to trace the change of the chemical states from the outer surface to the inside of the sample. The depth profiles of Mo_2N prepared from different precursors after HDN of indole at 673 K for 10 h are given in Fig. 10. Spectra of O_{1s}, N_{1s}, C_{1s}, Mo_{3d}, and P_{2p} levels were recorded. O_{1s} profiles show that the amount of oxygen gradually decreased as the cycles of Ar^+ bombardment increased, indicating the gradual decrease in its concentration from the outer to the inner surface. However, it did not disappear even though 20 nm surface was removed, indicating that oxygen can diffuse into the lattice interstices of the deeper layers during passivation. The core level of N_{1s} was overlapped with that of Mo_{2p}. After deconvolution, the amount of nitrogen was also found to decrease along the depth of the surface. Carbon was deposited only on the very surface within 4 nm of depth. The Mo_{3d} level of the outer surface were triplet while it turned to doublet in the inner surface for all the samples. The P_{2p} peak profiles of P-containing catalysts were similar with a peak at the binding energy of 134.0 eV whose intensity decreased along the depth of the surface and another peak at 130.0 eV which emerged in the inner surface. The component with higher binding energy of about 134.0 eV can be assigned to the surface phosphate while that with lower binding energy at about 130.0 eV to a phosphide form (29, 30). It seems unlikely that unhydrolyzed phosphorus oxides (P_2O_5) would exist on our samples since it would have been associated with the water formed during the TPR process. Furthermore, all the catalysts have been exposed to air containing moisture in order to get passivated prior to XPS measurements.

The ratios of XPS peak areas for Mo_2N prepared from different precursors before and after reaction are listed in Table 2. No evident variation of C_{1s}/Mo_{3d} was observed on the surfaces of different samples after HDN reaction. Along the depth of the surface the amount of phosphorus decreases drastically in P-containing catalysts, indicative of the segregation of phosphorus to the surface. In

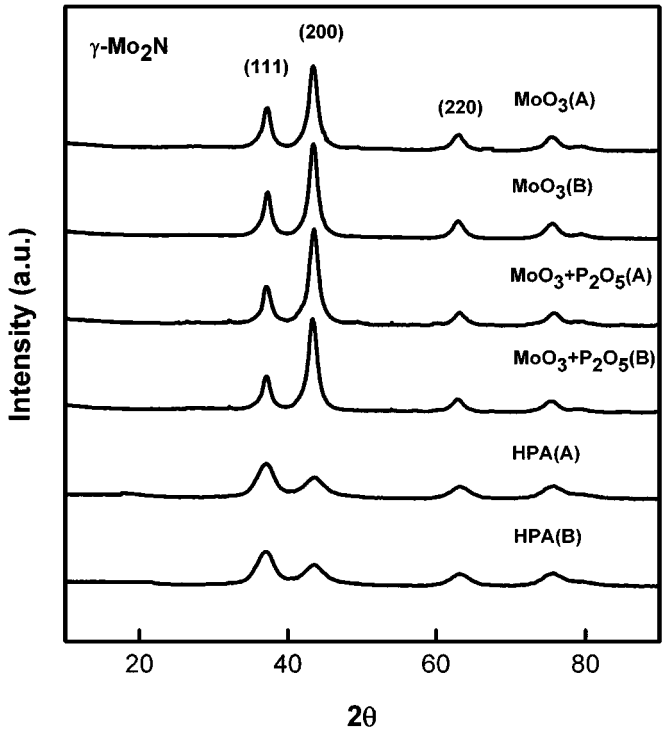

FIG. 7. X-ray diffraction patterns of Mo_2N prepared from different precursors before (B) and after (A) indole HDN reaction at 673 K for 10 h.

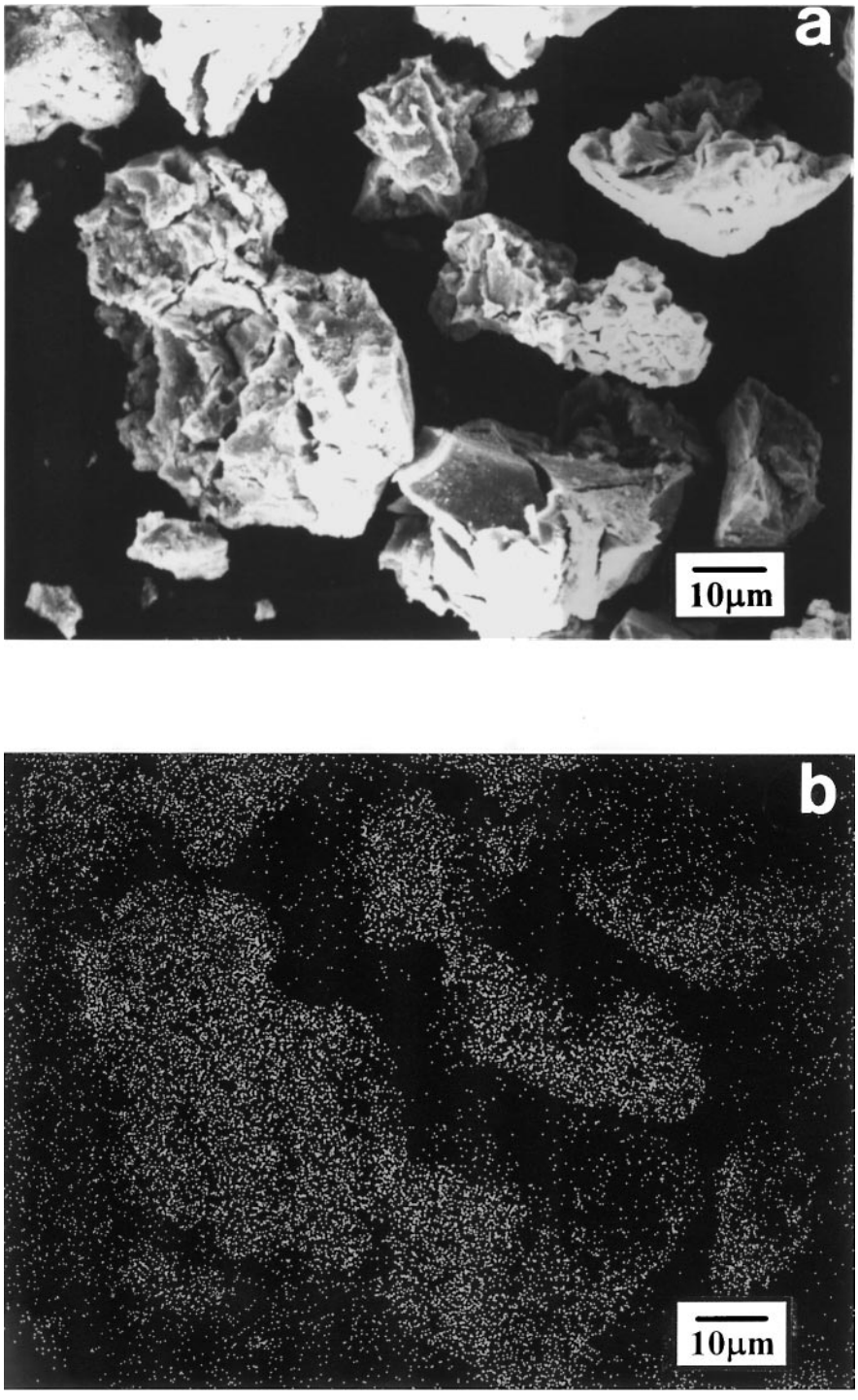

FIG. 8. Electron probe microanalysis (EPMA) of Mo_2N prepared from HPA after HDN of indole at 673 K for 10 h: (a) SEM image of the area analyzed and (b) phosphorus distribution.

terms of the XRD patterns, the bulk structure is Mo_2N for all the samples and it did not change after reaction. After deconvolution of the overlapped N_{1s} and Mo_{2p} peaks, the appreciable decrease of N_{1s}/Mo_{2p} ratios from the outer to the inner surface demonstrates that there was a great amount of amorphous nitrogen on the surface for all the samples. The N_{1s}/Mo_{2p} ratio after heavy sputtering showed the value closed to the stoichiometry of Mo_2N ($\sim$0.5). The excess nitrogen in fresh samples must come from the preparation step. In the case of Mo_2N prepared from MoO_3, the

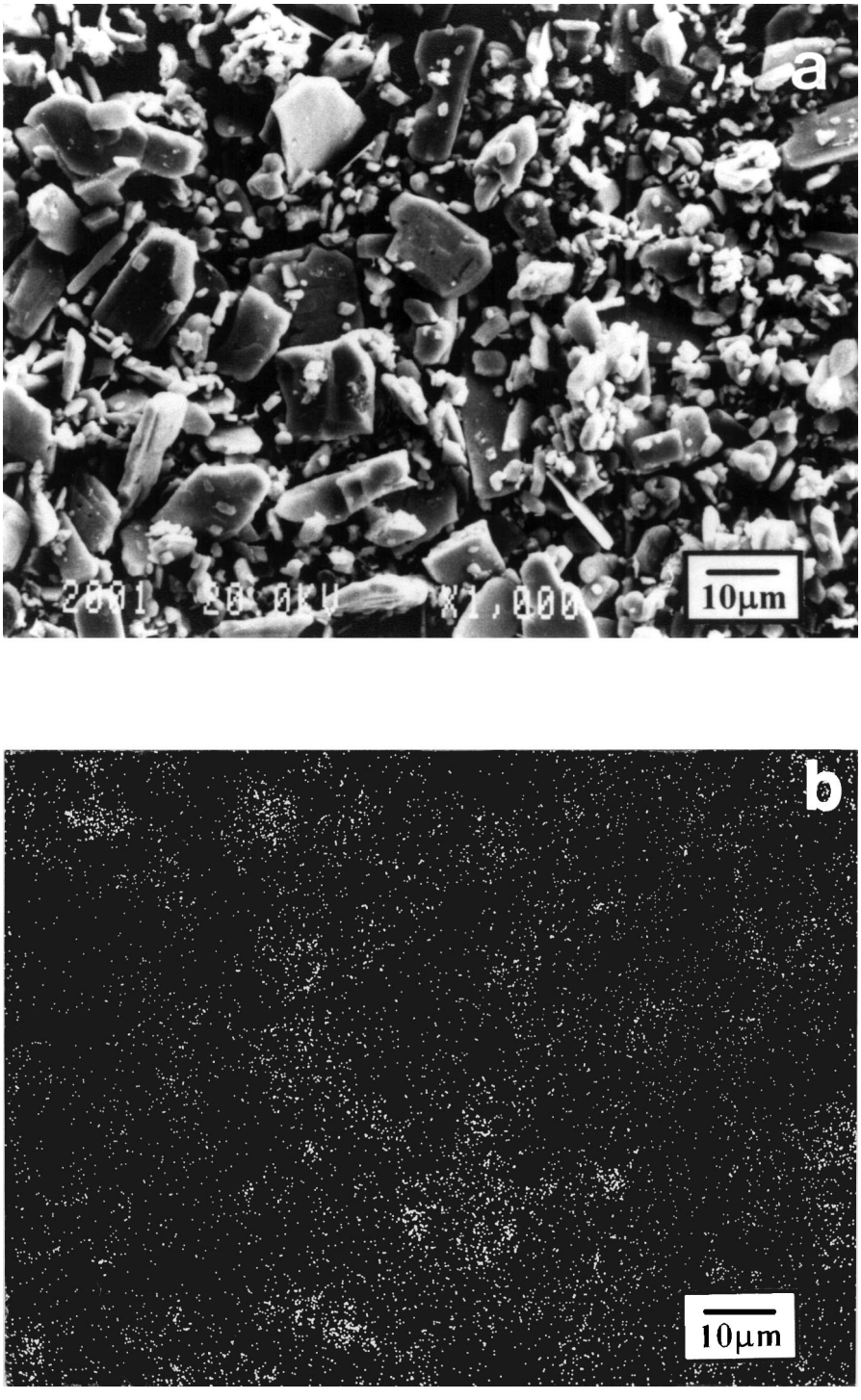

FIG. 9. Electron probe microanalysis (EPMA) of Mo_2N prepared from $MoO_3 + P_2O_5$ after HDN of indole at 673 K for 10 h: (a) SEM image of the area analyzed and (b) phosphorus distribution.

slight decrease of N_{1s}/Mo_{2p} after reaction probably resulted from removal of surface nitrogen by H_2 at 673 K. It appeared that HDN of indole did not increase the amount of N on the surface of pure Mo_2N. In contrast, the significant increase of N_{1s}/Mo_{2p} after reaction over Mo_2N derived from $MoO_3 + P_2O_5$ indicated the heavy deposition of nitrogen on the catalyst. The deposits of nitrogen species on HPA-derived Mo_2N were less significant than that of $MoO_3 + P_2O_5$ probably because of its smaller surface area.

TABLE 2

Ratios of XPS Peak Areas for Mo_2N Prepared from Different Precursors

Precursors	P_{2p}/Mo_{3d}			N_{1s}/Mo_{2p}			C_{1s}/Mo_{3d}		O_{1s}/Mo_{3d}		
	a	b	c	a	b	c	a	b	a	b	c
HPA	0.015	0.015	0.0019	3.8	3.9	0.64	0.082	0.11	0.41	0.37	0.14
MoO_3	—	—	—	3.9	3.0	0.49	0.12	0.092	0.33	0.27	0.13
$MoO_3 + P_2O_5$	0.027	0.016	0.0077	3.0	5.6	0.65	0.093	0.12	0.37	0.46	0.14

Note. a, before HDN reaction; b, after HDN of indole at 673 K for 10 h; c, after sputtering away 20 nm of b.

Figure 11 shows blowup of Mo_{3d} spectra of two precursors, MoO_3(a) and HPA(b), and Mo_2N prepared from different precursors before (c–e) and after (f–h) HDN of indole. The Mo_{3d} spectra of precursors MoO_3 and HPA typically consist of two envelopes centered at 232.6 and 235.8 eV, which represent the characteristic doublet Mo_{3d} of Mo^{6+}. However, all the Mo_{3d} levels of produced Mo_2N catalysts comprised triplet peaks. The complexity of Mo_{3d} peaks revealed the extreme heterogeneity of Mo species on the surface of Mo_2N. We did not try to decompose the Mo_{3d} peaks since they were poorly resolved following the deconvolution rules (28, 31). The complication of Mo_{3d} would make the curve fitting of more personal preference and of less physical meaning even though it could be decomposed. We simply compared the area of Mo_{3d} peak with $3d_{5/2}$ centered at 229.0 ± 0.2 eV to the total area of Mo_{3d} since the intensity of this peak was quite different among these catalysts both on the outmost surface and it remained in the inner layers after sputtering. The Mo_{3d} spectra with $3d_{5/2}$ at 229.0 eV were deconvoluted (Fig. 12, shaded areas) by the constraints that Mo_{3d} spin-obit doublet peaks have same full width at half maximum value (FWHM) with intensity ratio $I(3d_{5/2})/I(3d_{3/2})$ of 1.50 and splitting of 3.15 eV (28).

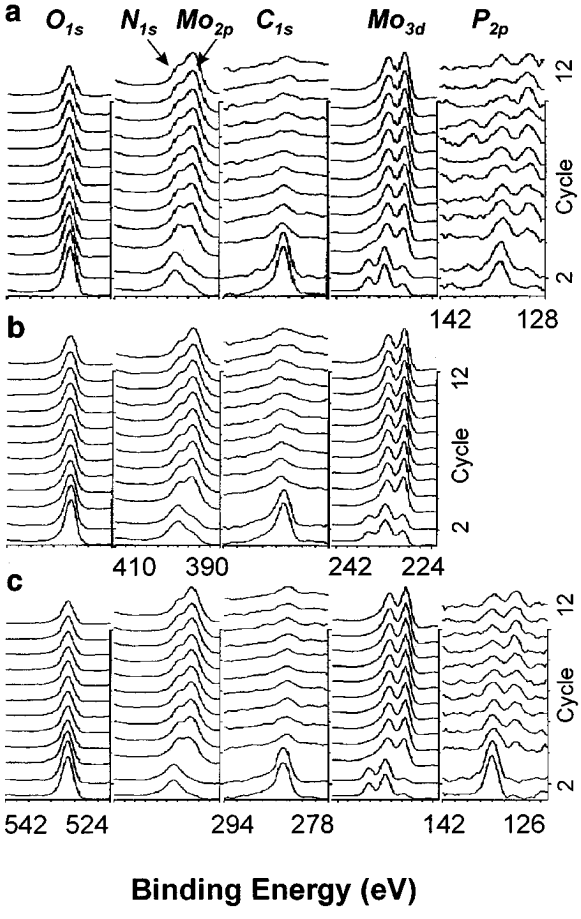

FIG. 10. Depth profiles of XPS analysis for Mo_2N prepared from different precursors after HDN of indole 673 K for 10 h. (a) Mo_2N prepared from HPA, (b) Mo_2N prepared from MoO_3, (c) Mo_2N prepared from $MoO_3 + P_2O_5$.

The ratios of Mo peak area of $3d_{5/2}$ at 229.0 eV to the total area of Mo_{3d} are listed in Table 3. The peak intensity of Mo_{3d} at 229.0 eV was relatively weak on fresh Mo_2N prepared from MoO_3 whereas it increased after HDN of indole. However, P-containing Mo_2N showed an opposite trend compared to that without P. The peak intensity of Mo_{3d} at 229.0 eV in the fresh catalyst increased with the addition of P_2O_5 but decreased considerably after HDN reaction. HPA-derived Mo_2N showed similar behavior.

DISCUSSION

The Pathway of Indole HDN Reaction over Mo_2N Prepared from Different Precursors

As shown in Figs. 2 and 3, indole HDN over Mo_2N prepared from different precursors showed similar product

TABLE 3

Ratios of Peak Area of Mo_{3d} with $3d_{5/2}$ at 229.2 ± 0.2 eV to the Total Area of Mo_{3d}

Precursor	a	b
HPA	0.34	0.28
MoO_3	0.27	0.39
$MoO_3 + P_2O_5$	0.39	0.18

Note. a, before HDN reaction; b, after indole HDN reaction at 673 K for 10 h.

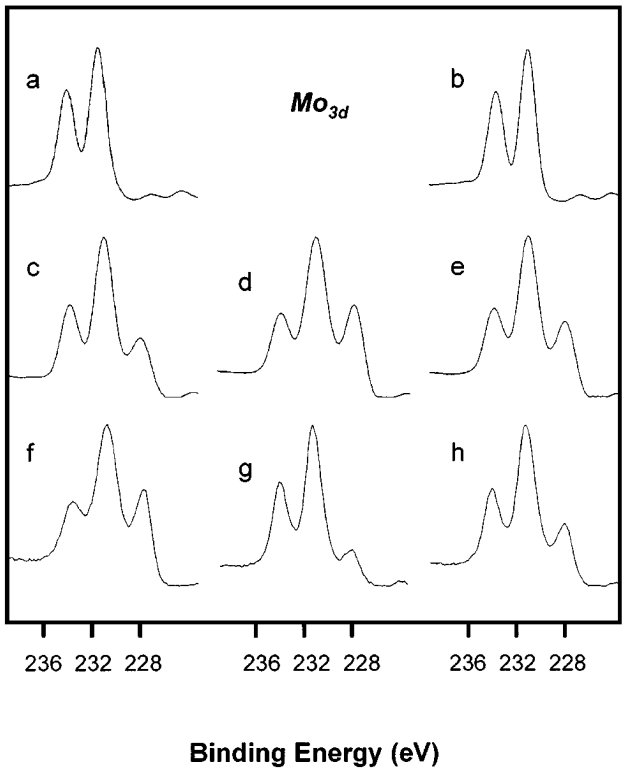

FIG. 11. X-ray photoelectron spectra of Mo_{3d} profiles of precursor (a) MoO_3 and (b) HPA, and Mo_2N prepared from (c) MoO_3, (d) $MoO_3 + P_2O_5$, (e) HPA before reaction, Mo_2N prepared from (f) MoO_3, (g) $MoO_3 + P_2O_5$, (h) HPA after indole HDN reaction at 673 K for 10 h.

distribution with a wide range of temperatures, implying that reaction might follow a similar pathway whether the catalyst contained phosphorus or not.

Based on the reaction pathway proposed by Oyama for HDN of quinoline (23) and that of Abe's (25), and considering the varying product distribution with temperature, a possible sequence of indole HDN reaction is shown in Fig. 13. The first step is the hydrogenation of heteroatom-containing ring to indoline where rapid equilibrium is reached. The second step is the cleavage of C–N bond in the saturated heterocyclic ring, leading to the formation of ethylaniline. The third step is the simultaneous hydrogenolysis of C–C and C–N bonds of ethylaniline, resulting in the formation of methylaniline and aniline, and the loss of NH_2 group to ethylbenzene and then to methylbenzene and benzene. At higher temperatures, hydrocracking is also involved in the reaction leading to the formation of saturated hydrocarbons.

The product distribution with time on stream in Figs. 5 and 6 could also be understood in terms of the proposed reaction scheme. At the beginning of the reaction when many fresh active sites are available, all the hydrogenolysis proceeds completely. Consequently, nearly all the products are hydrocarbons. However, when those highly active sites are poisoned during the reaction, the hydrogenolysis of C–N bonds is much retarded, leading to the increase of aniline group compounds and decrease of hydrocarbons. In the case of HPA derived-Mo_2N the amount of aniline group compounds also decreased when the active sites were heavily poisoned at the later stage of the reaction (Fig. 5c).

Beneficial Effect of Phosphorus for Indole HDN Reaction

Mo_2N is an active catalyst for indole HDN reaction showing comparable reaction rates to that of Mo–Ni/γ-Al_2O_3 for the same catalyst weight. Mo_2N prepared from $MoO_3 + P_2O_5$ and HPA showed higher reaction rates than that from MoO_3, implying P played an important role in this reaction. The measurements of BET surface areas showed that P-containing Mo_2N possessed lower surface areas and that the surface areas decreased after HDN reaction over all the catalysts especially in the case of HPA (Table 1). The decreases in surface area after reaction are in agreement with the observations made for P-containing Mo-based alumina catalysts (14). As mentioned in the previous paper (32), the loss of surface area for fresh P-containing catalysts seemed to result from pore and site blocking due to the addition of phosphorus. Thus, a negative effect of phosphorus on catalytic performance might be expected. However, the results turned out to be the opposite. Addition of phosphorus promoted HDN of indole, particularly at the beginning of the reaction and at lower temperatures. Apparently, the negative influence on the surface has been overshadowed by its positive effect. Moreover, the intrinsic promotional effect of P must be much greater than observed because of substantially lower surface areas of P-containing catalysts.

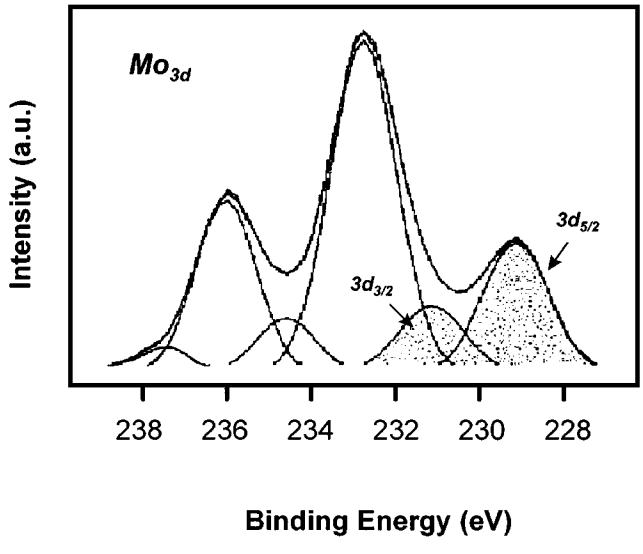

FIG. 12. Curve fitting of Mo_{3d} for Mo_2N prepared from HPA after HDN of indole at 673 K for 10 h.

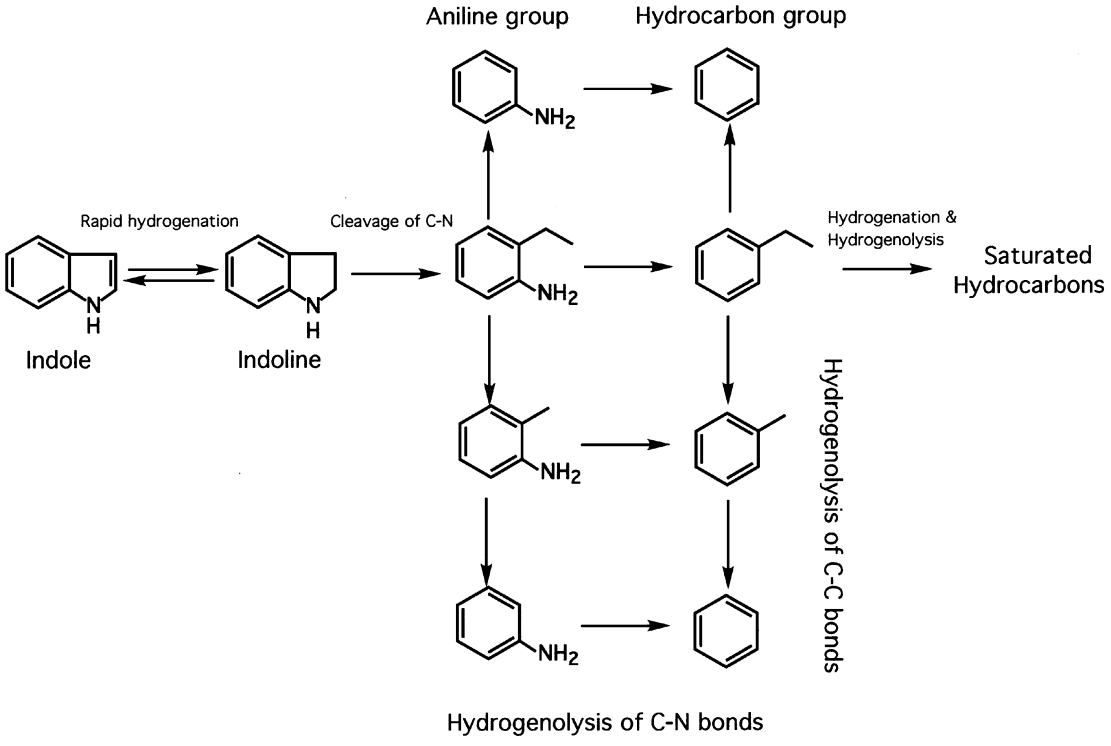

FIG. 13. Reaction pathway of HDN of indole over Mo_2N.

Deactivation of Catalysts

As shown in Table 1, the surface area decreased after HDN of indole for all the catalysts. This appears to be a main cause of deactivation over Mo_2N. In the case of P-containing Mo_2N, the deactivation was more evident due to the relatively greater loss of surface area.

Coking is believed to be one of the primary mechanisms for the deactivation of hydrotreating catalysts. It is well known that coke is formed via a carbenium ion and surface acidity is responsible for coking. In the case of $Mo(P)/Al_2O_3$ catalysts, it has been understood that surface acidity of alumina is reduced by multiple bonds formed between phosphorus and alumina and thus coking is considerably reduced (13).

In Mo_2N catalysts there was no significant difference of carbon content in these samples. It seems untenable to ascribe the deactivation of P-containing catalysts to their slightly higher carbon levels. A quantitative analysis of XPS results (Table 2) provided some clue to the problem. The only slight difference of C_{1s}/Mo_{3d} among these samples suggests that carbon deposition on the surface was not the factor responsible for different stability of these catalysts in HDN of indole. Almost all of carbon was removed after sputtering away 2 nm surface, indicating that accumulation of carbon was limited only to the outer surface (Fig. 10).

When considering the correlation between the amount of nitrogen with the catalytic performance, it appears that nitrogen deposits are responsible for the deactivation of indole HDN over P-containing Mo_2N. For Mo_2N prepared from MoO_3, activity decreased only slightly with time on stream. This may have come from the slight decrease of surface area. When P_2O_5 was added, the initial activity was markedly increased by the promotional effect of phosphorus although the surface area was reduced by pore blocking. However, it was easier to deactivate because of facilitated nitrogen deposition. When phosphorus lost its function by the nitrogen deposit, Mo_2N prepared from $MoO_3 + P_2O_5$ showed similar behavior to that of pure Mo_2N. In the case of HPA-derived Mo_2N, the loss of surface area during the reaction was greater, therefore, the activity decreased to the greater extent when the promotional effect of phosphorus was lost.

Role of Phosphorus

As given in Fig. 10, the well-separated components of P_{2p} levels of P-containing catalysts suggest that at least two distinct oxidation states of phosphorus are involved in the inner surface with a different binding energy of about 4 eV. However, the similar XPS profiles of P-containing Mo_2N catalysts implied that the environment of P may be the same regardless of precursors.

In investigation of Co–Mo–S, a proposed active phase in HDN and HDS over the commercial sulfided $Ni(Co)–Mo/Al_2O_3$, lower oxidation states other than single Mo^{6+} have been suggested to be the active species. In our cases, most probably Mo_{3d} with $3d_{5/2}$ at 229.0 eV coming from

molybdenum bonded with nitrogen serves as a signature of active species. The binding energy of phosphorus implies that it exists as a phosphate form combined with Mo. Phosphorus addition appears to contribute to the increased intensity of the Mo peak at 229.0 eV and thus to the increased initial HDN activity. However, it also seems to promote the deposition of nitrogen during HDN of indole and loses its favorable function as an activity promoter by being heavily adsorbed with nitrogen deposits. In the case of Mo_2N prepared from MoO_3, the increased intensity of the peak at 229.0 eV after reaction may result from the partial removal of adsorbed nitrogen species under hydrogen during the reaction.

CONCLUSION

Mo_2N is an active catalyst for indole HDN reaction. It gave comparable activity on the same weight basis to that of Mo–Ni/γ-Al_2O_3 but less hydrogen consumption. The initial activity of the indole HDN reaction was significantly increased by adding phosphorus in the catalysts despite its pore and site blocking effects. The beneficial effort was quite obvious at the beginning of reaction. However, P-containing Mo_2N catalysts lost activity more readily than Mo_2N itself. The deactivation did not result from carbon but probably caused by nitrogen deposits from indole and loss of surface area. The bulk structure and morphology of the Mo_2N catalysts were not changed after indole HDN reaction. The reaction pathway appeared not altered by adding phosphorus.

REFERENCES

1. Haresnape, J. N., and Morris, J. E., British Patent 701217 (1953).
2. Colgan, J. D., and Chomitz, N., U.S. Patent 3 287 280 (1966).
3. Mickelson, G. A., U.S. Patent 3 749 663 (1973a).
4. Pine, L. A., U.S. Patent 3 904 550 (1975).
5. Voorhies, J. D., U.S. Patent 4 082 652 (1978).
6. Bouwens, S. M. A. M., Vissers, J. P. R., De Beer, V. H. J., and Prins, R., *J. Catal.* **112**, 401–410 (1988).
7. Hopkins, P. D., and Meyers, B. L., *Ind. Eng. Chem. Prod. Res. Dev.* **22**, 421 (1983).
8. Fitz, C. W., and Rase, H. F., *Ind. Eng. Chem. Prod. Res. Dev.* **22**, 40 (1983).
9. Eijsbouts, S., Van Gruythuysen, L., Volumer, J., De Beer, V. H. J., and Prins, R., *in* "Studies in Surface Science and Catalysis," Vol. 50, p. 79. Elsevier, Amsterdam, 1989.
10. Lewis, J. M., Kydd, R. A., Boorman, P. M., and Cvan Rhyn, P. H., *Appl. Catal. A* **84**, 103 (1992).
11. Cruz Reyes, J., Avalos-Borja, M., Lopez Corder, R., and Lopez Agudo, A., *Appl. Catal. A* **120**, 147–162 (1994).
12. Atanasova, P., and Halachev, T., *in* "New Frontiers in Catalysis, Proceedings of 10th International Congress on Catalysis" (L. Guczi *et al*., Eds.), Budapest, 1992; *in* "Studies in Surface Science and Catalysis," Vol. 75, Part C, p. 1907. Elsevier, Amsterdam, 1993.
13. Van Veer, J. A. R., Hendriks, P. A. J. M., Andrea, R. R., Romers, E. J. G. M., and Wilson, A. E., *J. Phys. Chem.* **94**, 5282–5285 (1990).
14. Lewis, J. M., and Kydd, R. A., *J. Catal.* **136**, 478–486 (1992).
15. Eijsbout, S., Van Gestel, J. N. M., Van Veen, J. A. R., De Beer, V. H. J., and Prins, R., *J. Catal.* **131**, 412–432 (1991).
16. Mangnus, P. J., Van Veen, J. A. R., Eijsbouts, S., De Beer, V. H. J., and Moulijn, J. A., *Appl. Catal.* **61**, 99–122 (1990).
17. Volpe, L., and Boudart, M., *J. of Solid State Chem.* **59**, 332 (1985).
18. Volpe, L., and Boudart, M., *J. of Solid State Chem.* **59**, 348 (1985).
19. Lee, J. S., Oyama, S. T., and Boudart, M., *J. Catal.* **106**, 125 (1987).
20. Lee, J. S., Volpe, L., Ribeiro, F. H., and Boudart, M., *J. Catal.* **112**, 44 (1988).
21. Ranhotra, G. S., Haddix, G. W., Bell, A. T., and Reimer, J. A., *J. Catal.* **108**, 24–39 (1987).
22. Lee, J. S., and Boudart, M., *Appl. Catal.* **19**, 207–210 (1985).
23. Schlatter, J. C., Oyama, S. T., Metcalfe. J. E., and Lambert, J. M., *Ind. Eng. Chem. Res.* **27**, 1648 (1988).
24. Markel, E. J., and Zee, J. W., *J. Catal.* **126**, 643–657 (1990).
25. Abe, H., and Bell, A. T., *Catal. Lett.* **18**, 1–8 (1993).
26. Nagai, M., Miyao, T., and Tuboi, T., *Catal. Lett.* **18**, 9–14 (1993).
27. Choi, J. G., Brenner, J. R., and Thompson, L. T., *J. Catal.* **154**, 33–40 (1995).
28. Briggs, D., and Seah, M. P. (Eds.), "Practical Surface Analysis Vol. 1—Auger and X-ray Photoelectron Spectroscopy," 2nd ed., p. 113 and p. 562. Wiley, New York, 1990.
29. Moulder, J. F., Stickle, W. F., Sobol, P. E., and Bomben, K. D., "Handbook of X-ray Photoelectron Spectroscopy," p. 233. Perkin-Elmer, Eden Prairie, MN, 1992.
30. Clark, D. T., and Fork, T., *Thin Solid Films* **70**, 261–283 (1980).
31. Gajardo, P., Pirotte, D., Defosse, C., Grange, P., and Delmon, B., *J. Electron Spec. and Related Phenomena* **17**, 121–135 (1979).
32. Li, S., and Lee, J. S., *J. Catal.* **162**, 76 (1996).